†E-mail: Stephen.Lancaster@geo.oregonstate.edu

GSA Bulletin; Month/Month 2010; v. 1xx; no. X/X; p. 000–000; doi: 10.1130/B30175.1; 7 figures; 1 table; Data Respository item 2010xxx.

[1]GSA Data Repository item 2010xxx, including a table describing detailed results of radiocarbon dating; figures showing stratigraphy of channel banks and radiocarbon sampling locations at C1262R, Cedar Creek mainstem, and Golden Ridge Creek mainstem; and detailed analysis of stratigraphy at sites of potential age reversals, is available at http://www.geosociety.org/pubs/ft2010.htm or by request to editing@geosociety.org.

Sediment reservoirs at mountain stream confluences: Dynamics and effects of tributaries dominated by debris-flow and fluvial processes

Stephen T. Lancaster†, Emily F. Underwood, and W. Terry Frueh
Department of Geosciences, Oregon State University, Corvallis, OR 97331, USA

ABSTRACT

Radiocarbon age estimates (N=68) from bank, terrace riser, and in-channel materials sampled from random locations near two channel confluences, a debris flow-dominated tributary to Cedar Creek and a fluvially dominated tributary to Golden Ridge Creek in the Oregon Coast Range, are proxies for sediment transit times through tributary and mainstem sediment reservoirs separated from one another by incised bedrock risers. Geomorphic, volumetric, stratigraphic, and sedimentologic data aided reservoir characterizations. Inferred transit time distributions for tributary deposits are right-skewed and heavy-tailed, indicating preferential evacuation of younger deposits. The debris flow fan is much larger than fluvial terraces on the other tributary, but mean transit times (± σ) in both reservoirs are similar: 1370 ± 2240 a and 1660 ± 2130 a for fan and terrace deposits, respectively. Whereas tributary deposits are much larger than mainstem deposits at both sites, mainstem deposits adjacent to the fan have a relatively short mean transit time of 442 ± 491 a, but mean transit time in mainstem deposits adjacent to the fluvial terrace is much greater: 3870 ± 6720 a. Reservoir flux estimates indicate that most (>60%) of the debris flow fan tributary's sediment yield enters fan storage, but only a small part (3%) of the fluvial tributary's yield enters storage at the confluence. Debris flows from the debris flow fan tributary apparently promote both greater storage of mainstem sediments and more rapid unbiased evacuation of mainstem deposits, whereas old mainstem deposits adjacent to the fluvial tributary have a much greater probability of preservation.

Keywords*:* Landform evolution, sediment supply, C-14, bedload, debris flows, Tyee Formation

INTRODUCTION

Stream channel and valley morphology strongly reflect the balance of sediment supplied to a system and the ability of the stream to transport it (Sklar and Dietrich, 1998; Hancock and Anderson, 2002). When short-term sediment fluxes are equal to long-term denudation rates, landscapes are considered to be in dynamic equilibrium or steady state, a concept firmly rooted in geomorphology (Gilbert, 1877; Hack, 1960; Reneau and Dietrich, 1991). In sediment budgets and evolution models for mountain landscapes, streams are often assumed capable to transport all sediment delivered to the fluvial system (e.g., Howard, 1994; Hovius et al., 1997). Where sediment supplies are stationary in a statistical sense, this assumption may hold over geologic timescales, but short-term sediment supplies to streams are typically variable even in steady-state landscapes (cf. Lancaster, 2008). This is particularly true in steep landscapes where debris flows intermittently deliver material to the fluvial system (Dietrich and Dunne, 1978, May and Gresswell, 2004). In these basins, sediment episodically delivered to channels must be temporarily stored and gradually released by fluvial erosion.

Prior studies in the steep, rugged slopes and deeply dissected valleys of the Oregon Coast Range have provided insight into the routing and storage of sediment at the transition between debris flow and fluvial processes in headwater landscapes (Dietrich and Dunne, 1978; Reneau et al., 1989; Benda and Dunne, 1997; Lancaster et al., 2001; Lancaster and Casebeer, 2007; Lancaster, 2008). In unchanneled hollows of the OCR, gradual soil creep and episodic debris flows triggered by shallow landslides (Montgomery and Dietrich, 1994; Iverson et al., 1997) constitute the dominant modes of sediment delivery to the fluvial system (Reneau and Dietrich, 1991). These debris flows scour channels to bedrock and entrain additional material as they travel (Stock and Dietrich, 2003). In the Pacific Northwest, a major component of debris flow material is wood, constituting on average 60% of debris flow volume (Lancaster et al., 2003). These woody debris flows typically stop upon arrival at confluences with larger, lower gradient streams or at other places where gradients decrease (Benda and Cundy, 1990) and form dams that impound sediment and subsequent debris flows (Lancaster et al., 2001; Lancaster and Grant, 2006). This mechanism delivers sediment to the system in episodic pulses, which are then gradually eroded by fluvial processes. Studies in the OCR indicate that long term (e.g., 1–10 ka) denudation rates are approximately equivalent to short term (e.g., 1–10 a) sediment yields, implying a steady-state landscape (Reneau and Dietrich, 1991; Bierman et al., 2001; Heimsath et al. 2001), although studies of longitudinal channel profiles and fill terraces underlain by abandoned bedrock straths call this finding of steady-state into question (Personius et al., 1993; VanLaningham et al., 2006).

Long- and short-term equivalence of sediment outputs suggests that headwater valleys in transitional zones store episodic inputs of sediment from debris flows, such as in debris flow fans and other deposits at tributary confluences, and this concept is well supported by field studies (e.g., Dietrich and Dunne, 1978; Sutherland et al., 2002; Lancaster and Casebeer, 2007) and explicitly incorporated in sediment routing models (e.g., Benda and Dunne, 1997; Lancaster et al., 2001, 2003; Lisle and Church, 2002; Malmon et al., 2003). (Note our use of "debris flow fan" rather than the more common "alluvial fan" to emphasize debris flow as the genetic process for these steep fans at the debris flow-fluvial transition.) The resulting time lag between sediment delivery and removal in these steep basins complicates sediment movement from hillslopes, through the headwater network dominated by debris flows (e.g., Stock and Dietrich, 2003), to the fluvial system. A complete understanding, then, necessitates identification of the various storage reservoirs in headwater landscapes and quantification of their sediment routing characteristics. For sediment in these reservoirs, transit times, i.e., the times between deposition and evacuation (cf. Bolin and Rodhe, 1973), can illuminate effects of different deposition and evacuation processes (e.g., Eriksson, 1971; Bolin and Rodhe, 1973; Dietrich et al., 1982; Nakamura and Kikuchi, 1996; Malmon et al., 2003; Lancaster and Casebeer, 2007).

Transit times of sediments exiting a reservoir likely depend on deposition and evacuation processes. If evacuation processes favor older sediments (e.g., if new deposition on an alluvial or debris flow fan typically forces channel avulsion to older parts of the fan), the transit time distribution might be symmetrical about a non-zero peak, and the average sediment age (i.e., mean time spent in reservoir so far) would be less than the average (mean) transit time. If evacuation processes are indiscriminate with respect to age (i.e., the “well-mixed” case, where all sediments have equal probability of evacuation), transit time and age distributions would be represented by identical exponential functions, and mean age would equal mean transit time. Lancaster and Casebeer (2007) found such a case in a valley reach where debris flow fans and associated alluvial impoundments dominated sediment storage and fluvial processes dominated evacuation. If evacuation processes favor younger sediments, the transit time distribution would again be right-skewed, but with a so-called heavy tail (i.e., values approaching zero more gradually than an exponential) such as a power law, and mean age would be greater than mean transit time. Lancaster and Casebeer (2007) found such a case in a valley reach where debris flows typically scoured the valley bottom’s center and left older, higher deposits at the sides.

Applying this conceptual framework to a sediment reservoir requires a definition of an “outlet” and some tracer that captures transit times of materials exiting the reservoir. For valley bottom or fan sediment reservoirs, materials in channel banks are most likely to be removed via bank erosion and most representative of materials recently evacuated via channel incision. If, as we assume, mean transit time within the channel is much less than the mean transit time in off-channel storage, then ages of materials in those banks are proxies for transit times, and collecting materials from channel banks is analogous to collecting materials in a bucket at the reservoir outlet. Fragments of detrital charcoal and wood found in these banks serve as tracers that can be dated using radiocarbon techniques (e.g., Trumbore, 2000).

As in Lancaster and Casebeer (2007), this study employs a spatially dense volume- and bank area-weighted radiocarbon dating strategy in order to assess sediment reservoir characteristics in headwater catchments of the Oregon Coast Range. Whereas Lancaster and Casebeer (2007) compared two valley reaches (~1 km), this study compares more localized sediment reservoirs at two tributary confluences where incised bedrock risers exposed in mainstem channel banks allow differentiation between tributary deposits atop the higher bedrock surfaces and mainstem deposits on the lower bedrock surfaces. The two confluence sites in this study represent different tributary process dominance regimes, debris flow and fluvial, respectively, and similar, fluvially dominated mainstems.

STUDY AREA IN THE OREGON COAST RANGE

Field work was located at two tributary junction sites in the Tyee Formation of the Oregon Coast Range (Fig. 1). This formation consists of thickly bedded, shallowly dipping Eocene turbidite deposits with local igneous intrusions (Heller and Dickinson, 1985). The terrain at the field sites is steep and highly dissected by narrow valleys with, typically, flat valley bottoms and oversteepened sideslopes at valley bottom margins (Lancaster, 2008). Ridgelines have a relatively uniform elevation of about 500 m, and hillslope soil cover is typically thin (~ 0.5 m; Heimsath et al., 2001). Some studies suggest that Pleistocene–Holocene climate changes affected hillslope sediment production and supply to fluvial systems, effects inferred from terraces on many Coast Range streams (Reneau and Dietrich, 1991; Personius et al., 1993). Cool, wet winters and warm, dry summers characterize the present climate and produce the *Tsuga heterophylla* zone’s drought tolerant conifer forest east of the coastal fog belt (Franklin and Dyrness, 1973). Long-duration rainstorms during October to May combine with steep, high relief slopes to produce debris flows, typically where the roots of the dense forest have been weakened by tree mortality following fire, harvest, or pestilence (Long et al., 1998; Montgomery et al., 2000; Roering et al., 2003). Large trees and debris flows combine to form frequent valley bottom-spanning debris dams that impound streams and give them characteristically stepped longitudinal profiles (Lancaster et al., 2001, 2003; Lancaster and Grant, 2006). Typical of riparian zones in the OCR, thick understory vegetation reaches heights of 2–3 m at the sites and limits visibility. Both study sites are located within the Siuslaw National Forest.

Where streams are actively downcutting, valley margins are often oversteepened to produce features variously recognized as oversteepened toe slopes, inner gorges, and slot canyons (e.g., Densmore and Hovius, 2000; Lancaster, 2008), and this incision by the mainstem can also leave tributary outlets separated from mainstem valleys by bedrock steps or waterfalls. The Cedar Creek and Golden Ridge Creek sites are located at tributary confluences where the tributary channels have such bedrock steps at their confluences with the mainstem channels. These incised bedrock risers extend along the margins of the active strath surfaces of the mainstem channels and provide boundaries with which to differentiate tributary and mainstem deposits (Fig. 2). In each case, deposits overlie bedrock, and channels deeply incise those deposits, to bedrock in at least some places.

Cedar Creek is a sub-basin of the Siuslaw River basin (Fig. 1). The Cedar Creek site comprises a debris flow fan at the mouth of a right-bank tributary to Cedar Creek as well as the adjoining mainstem channel and valley bottom (Table 1 and Fig. 2). (Note that we follow the convention of denoting right and left banks with respect to the downstream direction in all cases.) The tributary splits into two distributary channels, both of which incise the distal fan to bedrock. Both (tributary) distributary channels have relatively small inset fills forming surfaces denoted T1 (Fig. 2): a narrow alluvial fill is adjacent to much of C1282R (for Cedar Creek tributary entering at 1282 m from the outlet on the right bank; see Fig. 2), and an apparent debris flow deposit splits two forks of the channel at the head of C1262R. For purposes of this study, the upper risers leading to the debris flow fan surface (DF in Fig. 2A) are considered part of the channel banks, because the T1 treads appear to be inundated during high flows. A bedrock riser forms the mainstem's right bank at the C1262R confluence (Fig. 2). The mainstem also incises the valley bottom deposits to bedrock for most of its fan-adjacent length. The area adjacent to the site was selectively logged prior to the advent of modern logging techniques, as evidenced by the presence of an abandoned road parallel to the mainstem (Fig. 2) and some tall stumps with spring board holes, but it has not been logged since 1902 (the period of Siuslaw National Forest records; Forest and Koenitzer, 2003). The fan surface and both channels all have steep gradients (Table 1).

Golden Ridge Creek (cf. Bigelow et al., 2007; "Wassen Creek" site of May and Gresswell, 2004) is a sub-basin of the Smith River (Fig. 1). The Golden Ridge Creek site comprises a left-bank tributary channel (GR1119L), the predominantly alluvial deposits adjacent to the tributary channel, the mainstem channel, and the valley bottom deposits adjacent to the mainstem channel (Table 1 and Fig. 2). A bedrock riser forms the mainstem channel's left bank at the tributary junction (Fig. 2). Approximately four meters of predominantly alluvial fill overlie bedrock on the tributary side of the riser. This terrace surface is denoted T2 (Fig. 2). The tributary channel has incised through these deposits to bedrock over most of the study length but has aggraded part of the reach, and these in-channel bars are denoted T0. There appears to be an additional inset fill terrace, denoted T1 (Fig. 2), although later scrutiny of these surfaces suggests that T1 is not an inset fill (Fig. 2). Side channels on T1 may instead be responsible for the T2 risers, a cut bank on the left-bank side, and a more gradual right-bank riser where gravelly alluvium is prevalent. Because the T1 tread surface has evidence of recent inundation, the T2 risers are also considered to be channel banks for the purposes of this study.

METHODS

Radiocarbon Sampling and Deposit Characterization

We characterized evacuation of stored sediment volumes through construction of transit time distributions from large numbers of radiocarbon age estimates of bank materials, which are the sediments most likely to be evacuated (as noted above, terrace risers above low, frequently inundated, inset, channel-adjacent fill surfaces are also included). Conventional stratigraphy-based approaches have been used effectively to reconstruct histories of fill and strath terrace formation (e.g., Personius et al. [1993] and Wegmann and Pazzaglia [2002], respectively) and fire and fire-related alluvial processes (e.g., Meyer et al., 1992, 1995), but for the purposes of this study, such a strategy might lead to biased transit time distributions by over-sampling readily accessible exposures with well-preserved stratigraphy in indurated deposits. For this reason, as in Lancaster and Casebeer (2007), sampling points were randomly located on channel banks and terrace risers, with point density effectively weighted by both deposit volume and vertical projection of bank and terrace riser area. For characterization of transit times in sediment reservoirs with irregular geometry, volume weighting provides proportional representation of all reservoir parts, and weighting by bank and riser area provides proportional representation of likely evacuation flux planes.

The sampling procedure comprised the following steps: (1) determine three-dimensional geometries of stored sediments; (2) choose random points within those geometries; (3) find channel locations closest to those points; and (4) eliminate points that are either too low (beneath channel beds) or too high (above channel banks or terrace risers). Finally, we recorded stratigraphy and sedimentology at each sampling location.

Surveys with hand level, compass, tape, and stadia rod provided three-dimensional geometries at each site (Fig. 2). The surveys comprised longitudinal mainstem and tributary channel profiles along channel centerlines, with channel widths and bank heights also recorded at survey points; and transects along lines encompassing the deposits: for Cedar Creek, two transects converged at the fan apex, and two more defined the fan's upstream and downstream limits (Fig. 2A); for Golden Ridge Creek, four parallel survey lines transected the tributary deposits and, along a perpendicular bearing, four more parallel lines transected the mainstem deposits (Fig. 2B). Surface geometries of the deposits were interpolated between transects. For the fan at the Cedar Creek site, only points on the upper fan surface were included in determining its geometry for determination of volume and sampling locations (i.e., transect points falling on tributary channel beds, inset fills, channel banks, or terrace risers were omitted). Planes defining lower boundaries of the tributary deposit volumes were determined from bedrock elevations (for the Cedar Creek fan, only a few points near the incised bedrock riser). Similarly, valley gradients defined slopes of planes setting lower boundaries of mainstem deposits. Incised bedrock risers defined the boundaries between tributary and mainstem deposits. For the Cedar Creek fan, the edge of the deposit on the valley wall side was defined by assuming 40° valley walls extended beneath the fan to meet the bedrock strath.

The valley bottom sediment volumes, on both sides of the bedrock risers (Fig. 2), were then populated with random sample points. Sample points were projected to the nearest bank or terrace riser and matched to tape distances along the channel surveys. Vertical heights of sample locations were projected to heights on channel banks and terrace risers relative to surveyed channel points along the channel centerline (similar to but not generally equivalent to the thalweg, especially in the larger, mainstem channels). Points falling above or below accessible banks or terrace risers were rejected in the field. At actual sample locations, fresh exposures on banks and risers were excavated by shovel to reduce the chance of sampling material sloughed off from above.

Excavation also allowed characterization of deposits by classification according to mechanisms of deposition following Collinson (1978): fluvial gravels are sorted, rounded, and clast-supported; fluvial fines are fine sedimentary layers often interbedded with organic material; and debris flow deposits typically have poorly sorted, angular, matrix-supported clasts. Additionally, for classification as fluvial gravels, evidence of fluvial deposition such as imbrication or stratification was sought because debris flows often rework fluvial deposits. In general, stratigraphy was recorded only in immediate vicinities of sampling locations because dense vegetation and collapsed bank and riser material made more extensive excavation infeasible. Instead, sections of banks and risers with nearby sampling locations (i.e., within 1–2 m horizontal distance) were targeted in order to ascertain, as possible, the stratigraphic relationships of the locations. Dateable material was found at all sample points, although boulders, logs, and filled burrows and root cavities in some cases necessitated taking samples from either the opposite banks or the nearest sediments allowing feasible sampling (always within a meter of the original point). Sampling was therefore not biased by the absence of material for sampling. Samples were examined under a microscope to identify characteristic features that allowed species classification (cell structure, resin canals, earlywood–latewood transition, and spiral thickenings; Hoadley, 1990).

Sediment samples for bulk-density measurements were taken at every third sample location with a soil probe, perpendicular to the bank. These samples were dried and weighed to determine dry bulk densities. Because the sample diameter was limited to 5 cm, larger grain sizes were not sampled, and bulk densities may represent minimum estimates.

All work at the Cedar Creek site took place in July and August 2006, and nearly all work at the Golden Ridge Creek site in August and September 2006. Due to lack of time in 2006, sampling locations were relocated and marked at the Golden Ridge Creek site in August 2008, based on the surveys and sedimentology, and detailed stratigraphy was recorded then and, in two cases, in August 2009.

Sample Age Distributions

Samples for radiocarbon dating were analyzed at the Accelerator Mass Spectrometer facility at the University of Arizona. Radiocarbon age estimates were calibrated with the OxCal program (Bronk Ramsey, 2001) and the IntCal04 and BombNH04 calibration curves (Hua and Barbetti, 2004; Reimer et al., 2004). The resulting probabilities were summed and normalized for each of the terrace and mainstem deposits to provide relative probability densities of sample age estimates and, thus, inferred transit-time distributions.

As found by Lancaster and Casebeer (2007), we expect the transit time distributions to be right-skewed with maxima at or near zero transit time. In such cases, shapes of the distributions' tails are particularly indicative of reservoir characteristics, and those shapes are best revealed in log-log plots of exceedance probability, i.e., probability of transit time greater than or equal to a given time. Calibrations of radiocarbon ages yield distributions of ages "before present" (B.P.), where "present" is, by convention, A.D. 1950. We obtained the best estimates of transit times for the exceedance distributions by shifting calibrated ages to times before the actual sampling year, A.D. 2006, and using the weighted mean calibrated age for each sample (cf. Telford et al., 2004).

For stored volumes with large enough numbers of samples (e.g., N>20), distribution shapes were characterized by fitting functions to the exceedance distributions.

Reservoir Fluxes

The mean transit time for sediments stored in a steady-state reservoir is termed the residence time by Eriksson (1971),

$$t_r = \frac{M_0}{F_0}, \qquad (1)$$

where M_0 is the total mass of the reservoir, and F_0 is the total flux rate through the reservoir. To estimate the long-term flux through the reservoir, we solve equation (1) for F_0, calculate M_0 from measured reservoir volumes and bulk densities, and use the mean of the bank deposit ages (i.e., the transit time proxies) for t_r. Flux through each reservoir is then compared to the contributing basin's sediment yield, estimated by assuming a uniform denudation rate of 0.1 mm/yr (e.g., Heimsath et al., 2001) over the contributing area and a weathered rock density of 2270 kg/m^3 (Anderson et al., 2002). Evaluation of the assumptions of steady-state over millennial timescales and that radiocarbon ages represent timing of deposition will be based on the results.

RESULTS

Deposit Age Estimates and Characterization

Age estimates at both sites imply a lack of recent disturbance (see GSA Data Repository Table DR1[1]). None of the tributary samples has post-bomb levels of radiocarbon. Only one sample from mainstem Golden Ridge Creek has a post-bomb level, and it is indicative of fluvial deposition about 50 years ago (weighted-mean calibrated age –5 yr B.P.; Table DR1 [footnote 1]; Fig. 2).

Samples associated with the tributary at Cedar Creek (N = 30) were primarily from debris flow deposits (N=19), and the others were nearly all fluvial gravels (N = 10) (Fig. 3; Fig. DR1 and Table DR1 [footnote 1]). Bouldery deposits commonly compose the tributary channel banks and the risers to the fan surface. Mainstem samples at Cedar Creek (N=5) also came substantially from debris flow deposits (N = 2) (Fig. DR2 and Table DR1 [footnote 1]).

In contrast, samples associated with the tributary at Golden Ridge Creek (N = 24) all came from fluvial deposits, about half each from fluvial gravels (N = 13) and fluvial fines (N = 11; Fig. 4; Table DR1 [footnote 1]). Debris flow deposits, some with boulders, were exposed in the T2 risers (Figs. 4 and 5). Mainstem samples at Golden Ridge Creek (N=8) all came from fluvial deposits, primarily fluvial gravels (N=6; Fig. DR3 and Table DR1 [footnote 1]).

Several pairs of sample ages appear to indicate age reversals, i.e., places where older samples appear to overlie younger samples, but detailed stratigraphic analysis resulted in the exclusion of only one sample from further analysis (see Supplementary Results in the GSA Data Repository [footnote 1]). For example, apparently age-reversed samples at 3.2 and 4.1 m distance in the left bank T2 riser at GR1119L are separated by an inferred buttress unconformity (Fig. 5), and both overlie an older sample (872 yr B.P.) from fluvial gravels at 2.9 m (Fig. 4). The oldest Cedar Creek tributary sample (right bank of C1282R, 18 m from the mainstem, 10,481 yr B.P.) came from debris flow sediment, likely of tributary origin, near bedrock at the distal end of the debris flow fan (Fig. 3; Table DR1 [footnote 1]). The nearest younger sample (left bank, at 24 m, 170 yr B.P.) came from a fluvial gravel deposit at a lower elevation in a shorter bank, probably from reworking by the mainstem or tributary (Fig. 3). Because fluvial gravels are absent in the column of the oldest deposit, these samples must be separated by an unconformity, either destroyed by the tributary channel or hidden beneath bank vegetation. The one sample excluded from further analysis, at 26.6 m in the right bank of T1 at GR1119L (1899 yr B.P.; Table DR1 [footnote 1]; Fig. 4), is from fluvial fines with backset bedding (i.e., dip upstream) upstream of a younger sample, at 24.4 m (923 yr B.P.; Table DR1 [footnote 1]; Fig. 4), such that the two are stratigraphically inverted.

Sediment Transit Times and Fluxes

The Cedar Creek debris flow fan is much larger than the Golden Ridge Creek tributary terrace deposits, but the two reservoirs have similar mean transit times (inferred from calibrated ages and calculated relative to the time of sampling in 2006; Table 1). The mainstem deposits are both much smaller than their tributary counterparts, but the relationships between tributary and mainstem mean transit times are different at the two sites: the Cedar Creek mainstem reservoir has a mean transit time much shorter than that of the debris flow fan, and the Golden Ridge Creek mainstem reservoir, due to two of its samples ($N = 8$) having ages greater than 10 ka, has a mean transit time much greater than that of the tributary terraces (Table 1).

Probability density functions of calibrated sample ages are right-skewed and imply that sediment transit times in these reservoirs are most likely nearly zero but can approach several millennia in all cases but the Cedar Creek mainstem (Fig. 6). These distributions show that the Cedar Creek debris flow fan is unique among sites in that the oldest samples all come from debris flow deposits, including one sample with a weighted mean calibrated age greater than 10,000 yr B.P. (Fig. 6A; Table DR1 [footnote 1]). At other sites, the oldest samples are from fluvial gravels, including two samples from mainstem Golden Ridge Creek with weighted-mean calibrated ages greater than 10,000 yr B.P. (Figs. 6B and 6D; Table DR1 [footnote 1]).

Only the tributary deposits had enough samples to warrant fitting functions to the calibrated age (before 2006), or inferred transit time, exceedance distributions (Fig. 7). With sample standard deviations substantially larger than sample means (Table 1), both distributions are well characterized by power-law functions with exponents between 0 and –1, and more poorly by exponential functions, for which mean and standard deviation are equal (Fig. 7). The distribution shapes are characteristic of all the data and therefore not significantly affected by any single calibrated age, even the oldest (e.g., weighted-mean calibrated age 10,481 yr B.P., or transit time 10,537 yr B.P. relative to A.D. 2006, for the Cedar Creek fan). Heavy-tailed transit time distributions such as these imply that evacuation probabilities are age-dependent: younger deposits are more likely to be evacuated. From Bolin and Rodhe (1973), we infer that mean ages of stored sediments are greater than mean transit times. Note that our calibrated ages provide estimates of transit times of sediments through the reservoirs and not ages of sediments stored in the reservoirs, because bank exposures may not be characteristic of all stored sediment.

Reservoir flux and contributing basin yield estimates indicate that the sediment reservoirs trap only small percentages of those yields, except for the Cedar Creek fan, which may have a trapping efficiency >90% (Table 1), if the fan's active volume, for which the inferred transit times are applicable, includes all sediment above an assumed bedrock strath at the elevation of the bedrock exposed at the fan's distal end. A lower, and likely more accurate, estimate of trapping efficiency includes only material above the present depth of tributary incision (Table 1). This lower estimate is similar to Benda and Dunne's (1997) estimated 60% of debris flow volumes entering fan storage at first- and second-order channel mouths (with a 10^4 m^2 threshold contributing area defining channel heads, the Cedar Creek tributary is a second-order channel). Both tributary deposits trap greater fractions of total yield than do adjacent mainstem deposits.

From flux estimates for the Cedar Creek debris flow fan, literature-derived debris flow volumes yield recurrence intervals of debris flow deposition on the fan. May (2002) found a relationship between deposited sediment volume and cumulative debris flow runout length: debris flows that travel farther accumulate more sediment. Assuming an average runout length, $L = A^{1/2}$, where A is contributing basin area (Table 1), debris flow sediment volume from May (2002) is 1800 m^3. Recurrence interval for debris flow deposition is then $T = V/F$, where V is volume and F is volume flux. Bulk density and lower and upper estimates of mass flux from Table 1 yield recurrence intervals of 110 a and 69 a, respectively, comparable to the apparent time since debris flow deposition on the fan from the youngest sample ages, ~150 ± 100 yr B.P. (Table DR1 [footnote 1], or ~200 ± 100 a before 2006), especially noting two things: the last major disturbance may have produced more than one debris flow, and the tributary channels' incision of this fan to greater depths than on other nearby debris flow fans on Cedar Creek indicates a greater than average time since disturbance. The latter sample ages are consistent with regional fire history (Impara, 1997).

DISCUSSION

Validity of Age Estimates

The predominance of ages younger than most of Gavin's (2001) inbuilt ages (~180–600 a) and the rarity of age reversals outside of the 2-σ analytic and calibration uncertainty suggest that most, but not all, of the sampled charcoal fragments were not stored in upstream reservoirs for significant times and, rather, represent times of deposition. Still, one substantial age reversal was found, and with a large number of samples, the possibility that other samples have substantial inherited ages cannot be ruled out. As with Gavin's (2001) study in British Columbia's coastal rainforest, rot resistant *Thuja plicata* at our sites can lead to large inbuilt ages. Note that our three oldest samples could not be identified as *Pseudotsuga menziesii*. Moreover, the large uncertainty in calibrated age inherent in samples younger than 400 yr B.P.

(e.g., large error bars in Fig. 7) makes apparent age reversals, or conversely the inferred lack thereof, in young samples impossible to verify (Reimer et al., 2004).

Potential errors in sampling site relocation at the Golden Ridge Creek site produced some uncertainty in the stratigraphy for that site and, therefore, some uncertainty around the finding, based on that stratigraphy, of only one significant age reversal at the site. Gaps in the stratigraphy at the Cedar Creek site add uncertainty to the ages at that site. It is likely that these uncertainties and those introduced by bioturbation by animal burrowing and tree uprooting, redeposition of older material, or burning of subsurface roots have led to substantial unquantified errors in sample ages and, possibly, to unidentified age reversals. Therefore, some caution in interpretation of the data is warranted due to unquantified uncertainties.

Most of the results of this study, however, are not contingent on one or two samples because of the large numbers of samples taken at the tributary sites, and age errors are therefore unlikely to affect either the inferred transit time distribution shapes or the major findings of this study. One exception is the effect of the two oldest samples in the study on the inferred mean transit time in mainstem Golden Ridge Creek and particularly the finding that it is substantially greater than in mainstem Cedar Creek. On the one hand, these ages might be suspect because of their rarity and the large age gap between them and the next oldest sample. On the other hand, the random placement of sampling locations and the right-skewed distributions of the ages of those samples imply that the oldest samples are inherently rare. In all cases, mean transit times presented here should be interpreted in the context of their large standard deviations (Table 1).

Steady-State Sediment Reservoirs in the Holocene

If these depositional features were growing, we might expect younger material to concentrate more distally or nearer the surface. However, the observed spatial distributions of transit times, where both young and old materials are distributed throughout (Figs. 2–5; Figs. DR1–DR3 [footnote 1]), indicate that debris flows and fluvial processes frequently incise these deposits. New material then fills the resulting accommodation spaces to produce mixed spatial distributions of transit times, as observed (e.g., Fig. 5).

These mixed spatial distributions suggest that the tributary deposit volumes, while variable over shorter times due to the dynamism of erosion and deposition processes, are generally stationary over timescales much longer than the recurrence interval of major disturbance (e.g., in the case of the fan, debris flow deposition). The abundance of relatively young material in both tributary deposits and the relatively young debris flow deposits found in mainstem Cedar Creek imply that depositional processes are active, and these depositional features are not shrinking. Also, these features apparently occupy all of valley accommodation space. Laterally, they extend from valley walls to incised bedrock risers. Vertically, the Cedar Creek fan cannot aggrade without backfilling into the tributary and aggrading the mainstem, because, at 10%, the fan is already just steep enough for debris flows to traverse it and reach the mainstem. The Golden Ridge Creek tributary deposit does show some evidence of recent vertical accretion near the top of T2 (at 15.4 m and 16.1 m; Fig. 4), but much older deposits found at similar heights imply that evacuation is at least keeping pace with deposition. Both mainstem channels are predominantly on bedrock, and the incised bedrock risers indicate active bedrock incision. It appears, then, that these deposits are not growing. Along the reach of Cedar Creek downstream of the study site, debris flow fans are prevalent, and all fill the valley except for relatively narrow widths of nearly level deposits occupied by the mainstem and bounded by incised bedrock risers in many cases. Along the reach of Golden Ridge Creek upstream of the study site, wide elevated deposits at tributary mouths are common. Some of these deposits may be deeper than at GR1119L, but the deposit thicknesses at the study site are typical. The possibility of nonstationary tributary deposit volumes cannot be excluded, but the available evidence supports, on average, stationary deposit volumes over long times (>1 ka) since at least the mid-Holocene and the applicability of a steady-state assumption in our analyses of transit-time distributions and reservoir fluxes.

Debris Flow Rates

Assuming that all debris flows in the Cedar Creek fan's contributing basin reach the outlet, our estimate of debris flow recurrence interval on the fan, 69–110 a, is equivalent to a debris flow rate of 0.065–0.10 $km^{-2}\ a^{-1}$. The latter range should be an underestimate, because debris flows in the Oregon Coast Range often deposit at contributing areas smaller than 0.14 km^2 and gradients greater than 10% (e.g., Lancaster et al., 2003). Yet, the above rate is substantially larger than Montgomery et al.'s (2000) estimate of 0.01–0.03 $km^{-2}\ a^{-1}$, based on 13 radiocarbon dates of basal colluvium in landslide-prone hollows (including 11 from Benda and Dunne [1987] and Reneau and Dietrich [1990]); and May and Gresswell's (2004) 0.016 $km^{-2}\ a^{-1}$, based on dendrochronology in 125 stream reaches with contributing areas of 0.1–1.1 km^2, both in similar sites in the Oregon Coast Range. May and Gresswell (2004) may underestimate the rate by missing older events overprinted by younger ones and events stopping upstream of their sites. Also, their estimate spans only 144 a, shorter than the average recurrence interval of forest fire (200 a; Long et al., 1998). Montgomery et al.'s (2000) estimate spans a long time but relies on the sampled locations representing landslide-prone sites.

Age Dependent Evacuation

For the tributary deposits, the heavy-tailed transit time distributions indicate that mechanisms of sediment evacuation favor removal of younger material and preservation of older material. For the Cedar Creek debris flow fan and Golden Ridge Creek tributary deposit, 50% of material is evacuated in 500 a and 800 a, respectively, but 10% of material remains for longer than 3 ka and 6 ka, respectively (Fig. 7). Preferential retention of older material has been observed in other studies that have dated valley floor deposits (Nakamura and Kikuchi, 1996; Lancaster and Casebeer, 2007). These studies suggest that material that resides on valley margins is visited by the channel less frequently and is thus more likely preserved. For the Golden Ridge Creek tributary deposit, all weighted mean calibrated sample ages greater than 1208 yr B.P. (excluding the 1899 yr B.P. sample) are from the T2 risers (Figs. 2 and 4). At the Cedar Creek fan, all samples from the inset fill (T1) and beneath the channel bed have sample ages less than 639 yr B.P. (Figs. 2 and 3; Fig. DR1 [footnote 1]).

Whereas we might expect, based on the results of Nakamura and Kikuchi (1996) and Lancaster and Casebeer (2007), that evacuation mechanisms would favor younger materials in the terrace deposits of the Golden Ridge Creek tributary, we might have expected a different result for the Cedar Creek debris flow fan, that avulsions on the fan might have favored evacuation of older materials. It may be that the great momentum of debris flows and their occasional scour of fan deposits favor formation of tributary channels along the central axis of the fan. The inset debris flow deposit within the area incised by C1262R (Fig. 2) indicates that individual debris flow deposition events do not necessarily completely fill volumes evacuated by channels between those events. If filling of those volumes and, therefore, channel avulsion are relatively rare, then it follows that evacuation of the oldest sediments would also be rare.

Arguably, the assumption that sampling locations are representative of recently or soon to be evacuated sediments is suspect for some samples. The right-bank T2 riser at GR1119L is not a cut bank, and while loose fluvial gravels are abundant on the surface, there are no obvious secondary channels adjacent to this riser. And, although locations within channel bars (T0) and beneath channel beds (B) in both tributaries may represent recently or soon to be evacuated deposits, these locations may not represent channel banks or terrace risers. Removal of these points from the exceedance distributions, however, does not fundamentally alter the results of this study. For both tributaries, removal of samples from the above suspect locations makes the heavy tails of the exceedance distributions even heavier: power-law exponents change from –0.718 to –0.673 (R^2 = 96%) for the Cedar Creek fan and from –0.745 to –0.666 (R^2 = 88%) for the Golden Ridge Creek tributary terraces. Age dependence of evacuation probabilities could therefore be even more pronounced than represented by the exceedance distributions of Figure 7.

Effects of Tributary Processes on Mainstem Sediment Reservoirs

For the mainstem deposit at Cedar Creek, the mean transit time inferred from five radiocarbon samples is one-third the inferred mean transit time of the fan deposits (Table 1). This difference likely reflects the smaller volume of the mainstem deposits and, perhaps, the greater transport capacity of the mainstem channel. In contrast, the mean transit time inferred from eight samples from mainstem deposits at Golden Ridge Creek is more than twice the inferred mean transit time for the tributary deposits, despite the smaller volume of the mainstem deposits, and nine times that of the mainstem deposits at Cedar Creek, again despite the much smaller volume of the mainstem deposits at Golden Ridge Creek (Table 1). The different mean transit times between the two mainstem sites depend on two samples with calibrated ages >10,000 yr B.P. from Golden Ridge Creek. While small sample sizes at both mainstem sites draw these two great ages into question, we believe they are significant based on the stratigraphy and the improbability of finding two such aberrations, of eight total samples, at different locations within the same relatively small sediment reservoir.

It appears, then, that the mainstem transit times reveal effects of different mechanisms for sediment evacuation between these two confluence systems. If the Golden Ridge and Cedar Creek mainstem transit times are representative of similar Oregon Coast Range confluences (Table 1), then mainstem deposits at confluences with relatively large (~1 km^2 or greater contributing area), low-gradient (~5% or less) tributaries have a greater likelihood of storing sediments for longer times than do mainstem deposits at relatively small (~ 0.1 km^2 or smaller contributing area), high-gradient (~10% or greater) tributaries, often with associated debris flow fans. For smaller, steeper tributaries, tributary debris flows may form mainstem deposits (as at Cedar Creek) that obliterate riparian vegetation and force mainstem channel avulsions. More frequent avulsions on valley bottoms not stabilized by riparian vegetation create more frequent and less biased access to different parts of relatively low-volume mainstem deposits and, therefore, higher probabilities of more rapid evacuation and lower probabilities of longer-term preservation. For larger, lower-gradient tributaries, however, debris flows rarely form mainstem deposits (none were conclusively identified in mainstem Golden Ridge Creek, but boulders were present in the bed and banks near the confluence). With fallen or floated large woody debris, therefore, as the dominant forcing mechanism (e.g., Montgomery et al., 2003), mainstem channel avulsions are less frequent and less often associated with destruction of stabilizing vegetation. Access to different parts of the mainstem reservoir, then, is less frequent and more biased, so preservation of old deposits, as found at Golden Ridge Creek, is more likely. The above mechanisms for evacuation versus preservation are independent of sediment transport capacity in the mainstem but, rather, dependent on probabilities of avulsions driven by debris flows, which are ultimately driven by landscape disturbances, such as forest fires, occurring in the surrounding watershed.

The above conceptual model of the effects of the tributaries on mainstem reservoir dynamics is reinforced by the reservoir flux analyses. While the Cedar Creek tributary is an order of magnitude smaller than the tributary at Golden Ridge Creek, the former tributary's fan traps a much larger fraction of its basin's yield (Table 1) and therefore has a much greater volume, so the fan's concomitant effect on the mainstem is greater. The trapping efficiency of the Cedar Creek mainstem reservoir, while small in absolute terms, is much greater than for the Golden Ridge Creek mainstem reservoir (Table 1). Where debris flows deposit, and especially where those deposits originate in tributaries, the deposits typically form debris dams that impound sediment (e.g., Lancaster and Grant, 2006; Lancaster and Casebeer, 2007). Valley bottom reaches with adjacent debris flow fans therefore have greater sediment-trapping efficiencies than do reaches without fans, and this trend is reflected in the differences between the two confluence sites studied herein.

CONCLUSIONS

Sediment transit times inferred from radiocarbon dating of channel banks, terrace risers, and subsurface in-channel deposits show that, for two sediment reservoirs associated with tributaries at their confluences with Cedar Creek and Golden Ridge Creek in the Oregon Coast Range, transit time distributions are right-skewed and heavy-tailed. These distributions indicate that evacuation probabilities are age dependent, such that young deposits are preferentially evacuated, while older deposits are preferentially preserved. So, while most sediments in each tributary deposit have transit times less than several hundred years, a significant fraction of sediments have transit times exceeding several millennia. These sediment reservoirs appear to be at steady state on time scales of 1000–5000 a and fill available accommodation space, which evolves in tandem with deposition and evacuation (Lancaster, 2008).

The dynamics of these two tributary reservoirs are otherwise different and effect different dynamics in their adjacent mainstem reservoirs. The Cedar Creek debris flow fan traps most of its tributary basin's sediment yield in the form of debris flow deposits with a recurrence interval on the order of 100 a (implying a debris flow rate 2–10 times larger than the estimates of Montgomery et al. [2000] and May and Gresswell [2004]), but some of these debris flows form deposits in the mainstem, where they both increase relative trapping efficiency of the mainstem reservoir by creating debris dams and decrease relative transit times of sediments through that reservoir by forcing channel avulsions. The Golden Ridge Creek tributary terrace deposit traps a relatively insignificant fraction of its basin's sediment yield, predominantly in the form of fluvial deposits, and has little effect on the mainstem reservoir, where based on the two oldest samples at Golden Ridge Creek, older deposits therefore have a much greater probability of preservation for much longer times (e.g., >10 ka).

Different sediment reservoir dynamics at these two confluences highlight the important effect of smaller, debris flow-delivering tributaries as sources of coarse sediment to larger streams and on the formation of sediment accumulations within those larger streams. Such coarse sediments are necessary for some aquatic species (e.g., spawning gravels for salmonid fishes) but, absent debris dams, may not accumulate in many mountain streams (Montgomery et al., 2003; Lancaster and Grant, 2006).

ACKNOWLEDGMENTS

This research was funded by the National Science Foundation (grant EAR-0545768). Andrew Meigs, Jay Noller, Gordon Grant, and Fred Swanson contributed insight and suggestions that improved the manuscript. Daniel Bida, Stephen Highland, and Jesse Johnson assisted with field work. Drew Coe, Grant Meyer, Dan Miller, and Susan Ivy Ochs provided helpful reviews.

REFERENCES

Anderson, S.P., Dietrich, W.E., and Brimhall, G.H., Jr., 2002, Weathering profiles, mass-balance analysis, and rates of solute loss: Linkages between weathering and erosion in a small, steep catchment: Geological Society of America Bulletin, v. 114, p.1143–1158.

Benda, L.E., and Cundy, T.W., 1990, Predicting deposition of debris flows in mountain channels: Canadian Geotechnical Journal, v. 27, p. 409–417, doi: 10.1139/t90-057.

Benda, L.E., and Dunne, T., 1987, Sediment routing by debris flow, *in* Beschta, R.L., Blinn, T., Grant, G.E., Swanson, F.J., and Ice, G.G., eds., Erosion and Sedimentation in the Pacific Rim: International Association of Hydrological Sciences Publication 165, p. 213–223.

Benda, L., and Dunne, T., 1997, Stochastic forcing of sediment routing and storage in channel networks: Water Resources Research, v. 33, p. 2865–2880, doi: 10.1029/97WR02387.

Bierman, P., Clapp, E., Nichols, K., and Caffee, M.W., 2001, Using cosmogenic nuclide measurements in sediments to understand background rates of erosion and sediment transport, *in* Harmon, R.S., and Doe, W.W., III, eds., Landscape Erosion and Evolution Modeling: New York, Kluwer Academic and Plenum Publishers, p. 89–115.

Bigelow, P.E., Benda, L.E., Miller, D.J., and Burnett, K.M., 2007, On debris flows, river networks, and the spatial structure of channel morphology: Forest Science, v. 53, p. 220–238.

Bolin, B., and Rodhe, H., 1973, A note on the concepts of age distribution and transit time in natural reservoirs: Tellus, v. 25, p. 58–62, doi: 10.1111/j.2153-3490.1973.tb01594.x.

Bronk Ramsey, C., 2001, Development of the radiocarbon calibration program OxCal: Radiocarbon, v. 43, p. 355–363.

Collinson, J.D., 1978, Alluvial sediments, *in* Reading, H.G., ed., Sedimentary Environments and Facies: Oxford, Blackwell Scientific Publications, p. 15–60.

Densmore, A.L., and Hovius, N., 2000, Topographic fingerprints of bedrock landslides: Geology, v. 28, p. 371–374, doi: 10.1130/0091-7613(2000)28<371:TFOBL>2.0.CO;2.

Dietrich, W.E., and Dunne, T., 1978, Sediment Budget for a small catchment in mountainous terrain: Zeitschrift für Geomorphologie, v. 29, p. 191–206.

Dietrich, W.E., Dunne, T., Humphrey, N.F., and Reid, L.M., 1982, Construction of sediment budgets for drainage basins, *in* Swanson, F.J., Janda, R.J., Dunne, T., and Swanston, D.N., eds., Sediment Budgets and Routing in Forested Drainage Basins: U.S. Department of Agriculture, Forest Service General Technical Report PNW-141, p. 5–23.

Eriksson, E., 1971, Compartment models and reservoir theory: Annual Review of Ecology and Systematics, v. 2, p. 67–84, doi: 10.1146/annurev.es.02.110171.000435.

Forest, Siuslaw National, and Koenitzer, W., 2003, Vegetation - Typed by photo interpretation (piveg), GIS data layer from http://www.fs.fed.us/r6/data-library/gis/siuslaw/documents/veg_000.zip, metadata from http://www.fs.fed.us/r6/data-library/gis/siuslaw/documents/veg_000.htm.

Franklin, J.F., and Dyrness, C.T., 1973, Natural vegetation of Oregon and Washington: U.S. Department of Agriculture, Forest Service General Technical Report PNW-8, 427 p.

Gavin, D. G., 2001, Estimation of inbuilt age in radiocarbon ages of soil charcoal for fire history studies: Radiocarbon, v. 43, p. 27–44.

Gilbert, G. K., 1877, Report on the Geology of the Henry Mountains: Washington, D.C., Geographical and Geological Survey of the Rocky Mountain Region, U.S. Government Printing Office, 160 p.

Hack, J. T., 1960, Interpretation of erosional topography in humid temperate regions: American Journal of Science, v. 258A, p. 80–97.

Hancock, G.S., and Anderson, R.S., 2002, Numerical modeling of fluvial strath-terrace formation in response to oscillating climate: Geological Society of America Bulletin, v. 114, p. 1131–1142.

Heimsath, A.M., Dietrich, W.E., Nishiizumi, K., and Finkel, R.C., 2001, Stochastic processes of soil production and transport: Erosion rates, topographic variation, and cosmogenic nuclides in the Oregon Coast Range: Earth Surface Processes and Landforms, v. 26, p. 531–552.

Heller, P.L., and Dickinson, W.R., 1985, Submarine ramp facies model for delta-fed, sand-rich turbidite systems: American Association of Petroleum Geologists Bulletin, v. 69, p.960-976.

Hoadley, R.B., 1990, Identifying Wood: Accurate Results with Simple Tools: Newtown, Connecticut, The Taunton Press, 223 p.

Hovius, N., Stark, C. P., and Allen, P. A., 1997, Sediment flux from a mountain belt derived by landslide mapping: Geology, v. 25, no. 3, p. 231–234, doi: 10.1130/0091-7613(1997)025<0231:SFFAMB>2.3.CO;2.

Howard, A. D., 1994, A detachment-limited model of drainage basin evolution: Water Resources Research, v. 30, no. 7, p. 2261–2285, doi: 10.1029/94WR00757.

Hua, Q., and Barbetti, M., 2004, Review of trophospheric bomb C-14 data for carbon cycle modeling and age calibration purposes: Radiocarbon, v. 46, p.1273–1298.

Impara, P., 1997, Spatial and Temporal Patterns of Fire in the Forests of the Central Oregon Coast Range [Ph.D. thesis]: Corvallis, Oregon State University, 354 p.

Iverson, R. M., Reid, M. A., and LaHusen, R. G., 1997, Debris-flow mobilization from landslides: Annual Review of Earth and Planetary Sciences, v. 25, p. 85–138, doi: 10.1146/annurev.earth.25.1.85.

Lancaster, S.T., 2008, Evolution of sediment accommodation space in steady-state bedrock-incising valleys subject to episodic aggradation: Journal of Geophysical Research, v. 113, p. F04002, doi: 10.1029/2007JF000938.

Lancaster, S.T., and Casebeer, N.E., 2007, Sediment storage and evacuation in headwater valleys at the transition between debris-flow and fluvial processes: Geology, v. 35, p. 1027–1030, doi: 10.1130/G239365A.1.

Lancaster, S.T., and Grant, G.E., 2006, Debris dams and the relief of headwater streams: Geomorphology, v. 82, p. 84–97, doi: 10.1016/j.geomorph.2005.08.020.

Lancaster, S.T., Hayes, S.K., and Grant, G.E., 2001, Modeling sediment and wood storage and dynamics in small mountainous watersheds, *in* Dorava, J.M., Montgomery, D.R., Palcsak, B.B., and Fitzpatrick, F.A., eds., Geomorphic Processes and Riverine Habitat: Washington, D.C., American Geophysical Union, Water Science and Application, v. 4, American Geophysical Union, p. 85–102.

Lancaster, S.T., Hayes, S.K., and Grant, G.E., 2003, Effects of wood on debris flow runout in small mountain watersheds: Water Resources Research, v. 39, p. 1168, doi: 10.1029/2001WR001227.

Lisle, T.E., and Church, M., 2002, Sediment transport-storage relations for degrading, gravel bed channels: Water Resources Research, v. 38, p. 1219, doi: 10.1029/2001WR001086.

Long, C.J., Whitlock, C., Bartlein, P.J., and Millspaugh, S.H., 1998, A 9000-year fire history from the Oregon Coast Range, based on a high-resolution charcoal study: Canadian Journal of Forest Research, v. 28, p. 774–787, doi: 10.1139/cjfr-28-5-774.

Malmon, D.V., Dunne, T. and Reneau, S.L., 2003, Stochastic theory of particle trajectories through alluvial valley floors: The Journal of Geology, v. 111, p. 525–542, doi: 10.1086/376764.

May, C.L., 2002, Debris flows through different forest age classes in the central Oregon Coast Range: Journal of the American Water Resources Association, v. 38, p. 1097–1113, doi: 10.1111/j.1752-1688.2002.tb05549.x.

May, C.L., and Gresswell, R.E., 2004, Spatial and temporal patterns of debris-flow deposition in the Oregon Coast Range, USA: Geomorphology, v. 57, p. 135–149, doi: 10.1016/S0169-555X(03)00086-2.

Meyer, G.A., Wells, S.G., Balling, R.C., Jr., and Jull, A.J.T., 1992, Response of alluvial systems to fire and climate change in Yellowstone National Park: Nature, v. 357, p. 147–150, doi: 10.1038/357147a0.

Meyer, G.A., Wells, S.G., and Jull, A.J.T., 1995, Fire and alluvial chronology in Yellowstone National Park: Climatic and intrinsic controls on Holocene geomorphic processes: Geological Society of America Bulletin., v. 107, p. 1211–1230, doi: 10.1130/0016-7606(1995)107<1211:FAACIY>2.3.CO;2.

Montgomery, D.R. and Dietrich, W.E., 1994, A physically based model for the topographic control on shallow landsliding: Water Resources Research, v. 30, p.1153–1171, doi: 10.1029/93WR02979.

Montgomery, D.R., Schmidt, K.M., Greenberg, H., and Dietrich, W.E., 2000, Forest clearing and regional landsliding: Geology, v. 28, p. 311–314, doi: 10.1130/0091-7613(2000)28<311:FCARL>2.0.CO;2.

Montgomery, D.R., Massong, T.M., and Hawley, S.C.S., 2003, Influence of debris flows and log jams on the location of pools and alluvial channel reaches, Oregon Coast Range: Geological Society of America Bulletin, v. 115, p. 78–88, doi: 10.1130/0016-7606(2003)115<0078:IODFAL>2.0.CO;2.

Nakamura, F., and Kikuchi, S., 1996, Some methodological developments in the analysis of sediment transport processes using age distribution of floodplain deposits: Geomorphology, v. 16, p. 139–145, doi: 10.1016/0169-555X(95)00139-V.

Personius, S.F., Kelsey, H.M., and Grabau, P.C., 1993, Evidence for regional stream aggradation in the central Oregon Coast Range during the Pleistocene–Holocene transition: Quaternary Research, v. 40, p. 297–308 , doi: 10.1006/qres.1993.1083.

Reimer, P.J., Baillie, M.G.L., Bard, E., Bayliss, A., Beck, J.W., Bertrand, C.J.H., Blackwell, P.G., Buck, C.E., Burr, G.S., Cutler, K.B., Damon, P.E., Edwards, R.L., Fairbanks, R.G., Friedrich, M., Guilderson, T.P., Hogg, A.G., Hughen, K.A., Kromer, B., McCormac, G., Manning, S., Bronk Ramsey, C., Reimer, R.W., Remmele, S., Southon, J.R., Stuiver, M., Talamo, S., Taylor, F.W., van der Plicht, J., and Weyhenmeyer, C.E., 2004, IntCal04 terrestrial radiocarbon age calibration, 0-26 cal kyr BP: Radiocarbon, v. 46, p. 1029–1058.

Reneau, S.L., and Dietrich, W.E., 1990, Depositional history of hollows on steep hillslopes, coastal Oregon and Washington: National Geographic Research, v. 6, p. 220–230.

Reneau, S.L., and Dietrich, W.E., 1991, Erosion rates in the southern Oregon Coast Range: Evidence for an equilibrium between hillslope erosion and sediment yield: Earth Surface Processes and Landforms, v. 16, p. 307–322, doi: 10.1002/esp.3290160405.

Reneau, S.L., Dietrich, W.E., Rubin, M., Donahue, D.J., and Jull, A.J.T., 1989, Analysis of hillslope erosion using dated colluvial deposits: The Journal of Geology, v. 97, p. 47–63, doi: 10.1086/629280.

Roering, J.J., Schmidt, K.M., Stock, J.D., Dietrich, W.E., and Montgomery, D.R., 2003, Shallow landsliding, root reinforcement, and the spatial distribution of trees in the Oregon Coast Range: Canadian Geotechnical Journal, v. 40, p. 237–253, doi: 10.1139/t02-113.

Sklar, L. and Dietrich, W.E., 1998, River longitudinal profiles and bedrock incision models: Stream Power and the influence of sediment supply, *in* Tinkler, K.J., and Wohl, E.E., eds., Rivers over Rock: Fluvial Processes in Bedrock Channels: Washington, D.C., Geophysical Monograph Series, v. 107, American Geophysical Union, p. 237–260.

Stock, J., and W. E. Dietrich, 2003, Valley incision by debris flows: Evidence of a topographic signature: Water Resources Research., v. 39, p. 1089, doi: 10.1029/2001WR001057.

Sutherland, D.G., Ball, M.H., Hilton, S.J., and Lisle, T.E., 2002, Evolution of a landslide-induced sediment wave in the Navarro River, California: Geological Society of America Bulletin, v. 114, p. 1036–1048, doi: 10.1130/0016-7606(2002)114<1036:EOALIS>2.0.CO;2.

Telford, R. J., Heegard, E., and Birks, H. J. B., 2004, The intercept is a poor estimate of a calibrated radiocarbon age: The Holocene, v. 14, p. 296–298, doi: 10.1191/0959683604hl707fa.

Trumbore, S.E., 2000, Radiocarbon geochronology, *in* Noller, J.S., Sowers, J.M., and Lettis, W.R., eds., Quaternary Geochronology: Methods and Applications: Washington, D.C., American Geophysical Union, Reference Shelf 4, , p. 41–60.

VanLaningham, S., Meigs, A., and Goldfinger, C., 2006, The effects of rock uplift and rock resistance on river morphology in a subduction zone forearc, Oregon, USA: Earth Surface Processes and Landforms, v. 31, p. 1257–1279, doi:10.1002/esp.1326.

Wegmann, K.W., and Pazzaglia, F.J., 2002, Holocene strath terraces, climate change, and active tectonics: The Clearwater River basin, Olympic Peninsula, Washington State: Geological

Society of America Bulletin, v. 114, p. 731–744, doi: 10.1130/0016-7606(2002)114<0731:HSTCCA>2.0.CO;2.

MANUSCRIPT RECEIVED 16 SEPTEMBER 2009

REVISED MANUSCRIPT RECEIVED 28 JANUARY 2010

MANUSCRIPT ACCEPTED 25 FEBRUARY 2010

Printed in the USA

FIGURE CAPTIONS

Figure 1. Location map of the Cedar and Golden Ridge (G.R.) Creek study sites in the central Oregon Coast Range. Dashed white lines outline contributing tributary basins in the insets. Stars indicate the locations of the tributary confluence sites.

Figure 2. Topographic and geomorphic maps of valley bottoms at Cedar Creek (A) and Golden Ridge Creek (B) field sites. Contours from surveys show elevations in meters height above ellipsoid (m.h.a.e.). Radiocarbon sample sites shown with weighted-mean calibrated ages (yr B.P.). Surveyed transects shown for reference. Surveyed channel centerlines omitted for clarity. Maps have different scales (indicated on axes). Distances on axes are relative to latitude-longitude coordinates of 43.9698283° N, 123.9157983° W at Cedar Creek and 43.7139303° N, 123.8722603° W at Golden Ridge Creek. Mainstem flow directions (arrows) shown with names. Tributary channels named with mainstem channel initial(s), distance (m) of confluence from mainstem outlet, and mainstem channel bank, right or left, at which tributary channel enters, e.g., C1282R is Cedar Creek tributary, 1282 m from the outlet, on the right bank. At Cedar Creek (A),

tributary valley enters at bottom, and tributary channels, C1262R and C1282R, flow from southeast to northwest; C1262R is disconnected from surface flow at its heads. At Golden Ridge Creek (B), arrow indicates flow direction of tributary channel, GR1119L; contours correctly show secondary channels on the T1 tread and mainstem deposit (MS) surface.

Figure 3. For western tributary at Cedar Creek site (C1282R; Fig. 2), stratigraphy of channel banks; longitudinal profiles of channel bed, inset terrace (T1), and debris flow fan surfaces (DF); and radiocarbon sample locations (white circles), shown with weighted mean calibrated ages (yr B.P.). Elevations in meters height above ellipsoid (m.h.a.e.) shown with 5× vertical exaggeration on right axis for left bank (top) and left axis for right bank (bottom). Right bank is shown as mirror image to facilitate comparison of banks. Distances shown relative to mainstem centerline at confluence. Points projected into the plane of the cross section. T1 is surface of inset fill. Lighter and darker shades of red and yellow used to differentiate finer and coarser facies of debris flow and fluvial gravel deposits, respectively.

Figure 4. For tributary at Golden Ridge Creek site (GR1119L; Fig. 2), stratigraphy of channel banks; longitudinal profiles of channel bed and terrace treads (T0, T1, T2); and radiocarbon sample locations (white circles), shown with weighted mean calibrated ages (yr B.P.). Elevations in meters height above ellipsoid (m.h.a.e.) shown with 3× vertical exaggeration on right axis for left bank (top) and left axis for right bank (bottom). Right bank is shown as mirror image to facilitate comparison of banks. Distances shown relative to mainstem centerline at confluence. Channel bed is bedrock except in reach adjacent to T0, an in-channel bar surface. Points projected into the plane of the cross-section; samples in T1 and T2 are generally several meters apart, and slope of right bank T2 riser is gradual (Fig. 2). T1 deposits, especially right bank, may

not be inset. Lighter and darker shades of red and yellow used to differentiate finer and coarser facies of debris flow and fluvial gravel deposits, respectively.

Figure 5. Photograph of one left-bank exposure of T2 riser on tributary at Golden Ridge Creek site (GR1119L; Figs. 2 and 6); stratigraphic interpretation (FF—fluvial fine; FG—fluvial gravel; DF—debris flow); and radiocarbon sample locations (white circles), shown with weighted-mean calibrated ages (yr B.P.). Sample from older deposit at 3.2 m (right side) separated by buttress unconformity from sample from younger deposit at 4.1 m (left side). An irregularly shaped cluster of rounded, imbricated boulders (FG) underlies both the older debris flow deposit (right side) and the younger fluvial gravels (left side).

Figure 6. Calibrated age (yr B.P.) probability density functions for (A) Cedar Creek tributary debris flow fan, (B) Golden Ridge Creek tributary terrace deposits, (C) Cedar Creek mainstem deposit, and (D) Golden Ridge Creek mainstem deposit. Each probability density function is normalized so that its integral is equal to one. Note that calibrated radiocarbon ages typically have multiple likely ages and exhibit asymmetry. This is a result of fluctuations in the atmospheric ^{14}C content reflected in the calibration curve. A peak in the distribution does not represent a single date, but rather the probability that one or more samples are of that age.

Figure 7. Calibrated age exceedance probability distributions for (A) Cedar Creek tributary debris flow fan and (B) Golden Ridge Creek tributary terrace deposits. Weighted-mean calibrated ages (white circles) are shifted to represent age relative to the sampling time, A.D. 2006, rather than the conventional age relative to A.D. 1950 (yr B.P., as in Figs. 2–6, Figs. DR1–DR3, and Table DR1), and are shown with their 2-σ errors (horizontal black solid lines). Power-

law and double exponential fits (gray lines) are shown with their equations, where *P* is exceedance probability, *t* is calibrated age (inferred to be transit time), and R^2 is the fraction of the variance of *P* explained by the fit.

TABLE 1. CHARACTERISTICS OF MAINSTEM AND TRIBUTARY FEATURES AT CEDAR CREEK AND GOLDEN RIDGE CREEK STUDY SITES

Site characteristics	Cedar Creek		Golden Ridge Creek	
	Tributary*	Mainstem	Tributary	Mainstem
Channel gradient	0.098	0.047	0.048	0.031
Valley gradient	-	0.050	-	0.035
Deposit volume (m^3)	2.4–3.6 × 10^4	6900	3200	980
Contributing area (km^2)	0.14	4.8	1.5	6.3
Bulk density (Mg/m^3)	1.1 ± 0.3	1.3 ± 0.3	1.2 ± 0.3	1.7 ± 0.2
Mass of deposits (Mg)	2.6–4.0 × 10^4	9000	3800	1700
Mean transit time ± σ (a, before 2006)†	1370 ± 2240	442 ± 491	1660 ± 2130	3870 ± 6720
Flux through reservoir (Mg/a)	19–29	20	2.3	0.44
Basin yield (Mg/a) §	32	1100	340	1400
Fraction of denudation stored	0.59–0.91	0.018	6.8 × 10^{-3}	3.1 × 10^{-4}

* Upper and lower ends of ranges correspond to upper and lower estimates of fan volume (see text).
† Sample mean and standard deviation are expressed here as $\mu \pm \sigma$, where μ is mean and σ is standard deviation, for conciseness only and not to represent the possible range of transit times, which cannot be negative.
§ Assumes bedrock lowering rate of 0.1 mm/a (e.g., Heimsath et al., 2001) and bedrock density of 2.27 Mg/m^3 (Anderson et al., 2002).

Figure 1

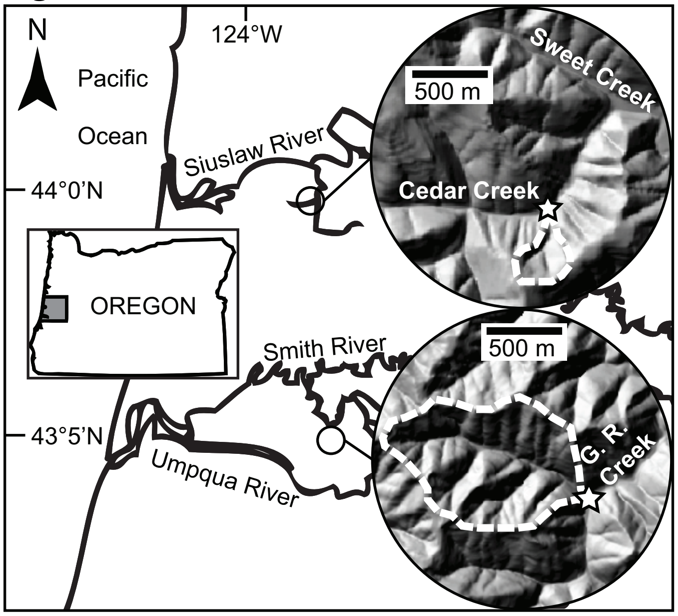
N
124°W
Pacific
Ocean
Siuslaw River
44°0'N
OREGON
Smith River
43°5'N
Umpqua River
500 m
Sweet Creek
Cedar Creek
500 m
G. R. Creek

805 **Figure 2**

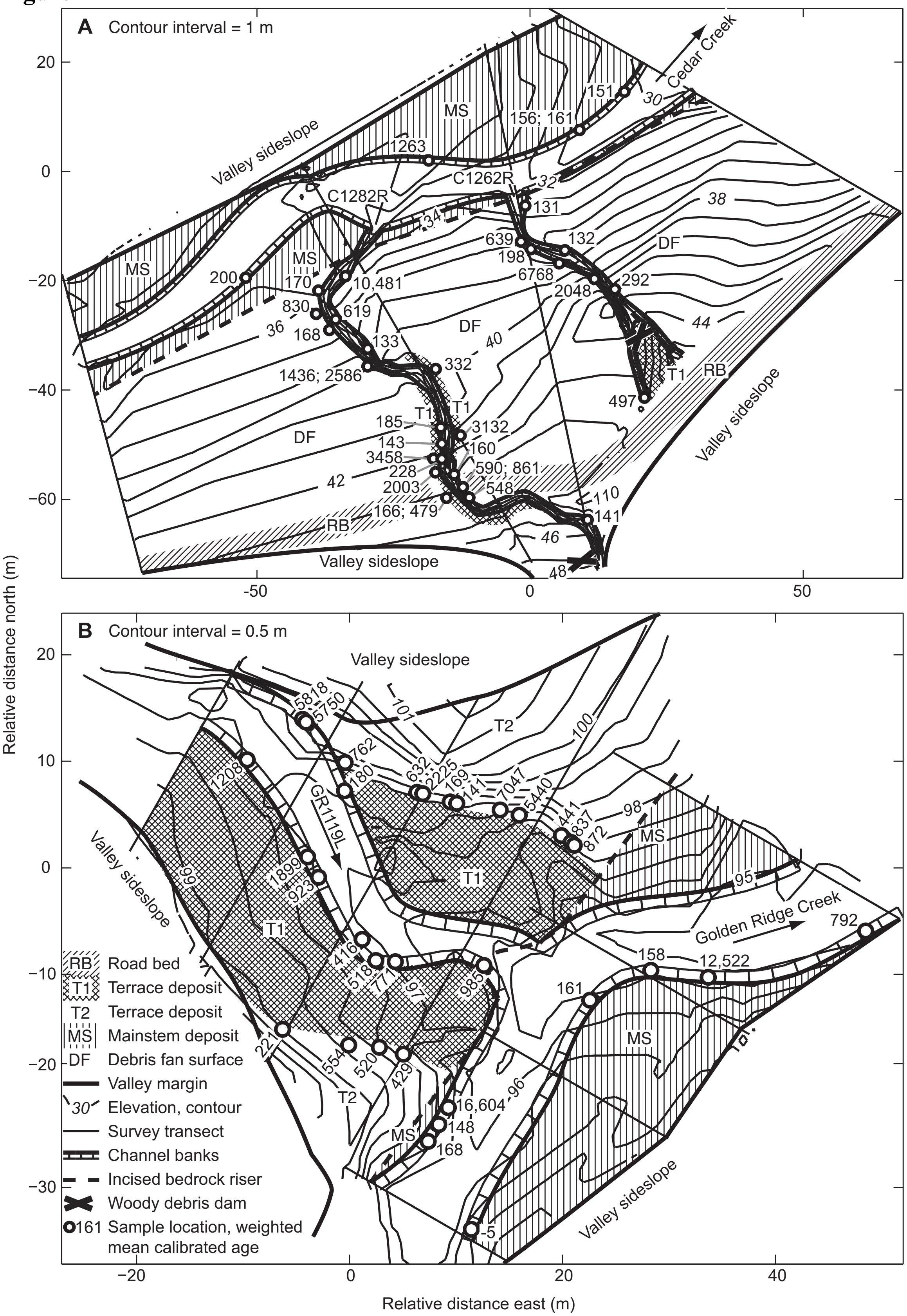

806
807

807 **Figure 3**

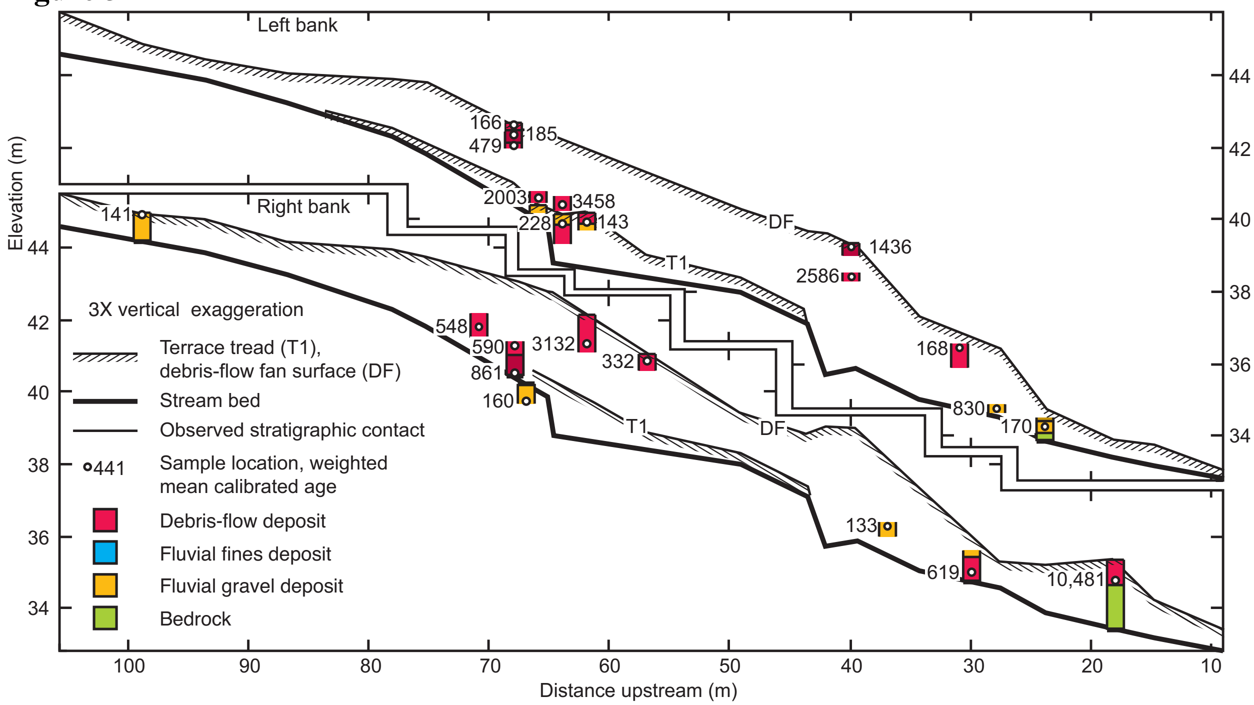

808
809

809 **Figure 4**

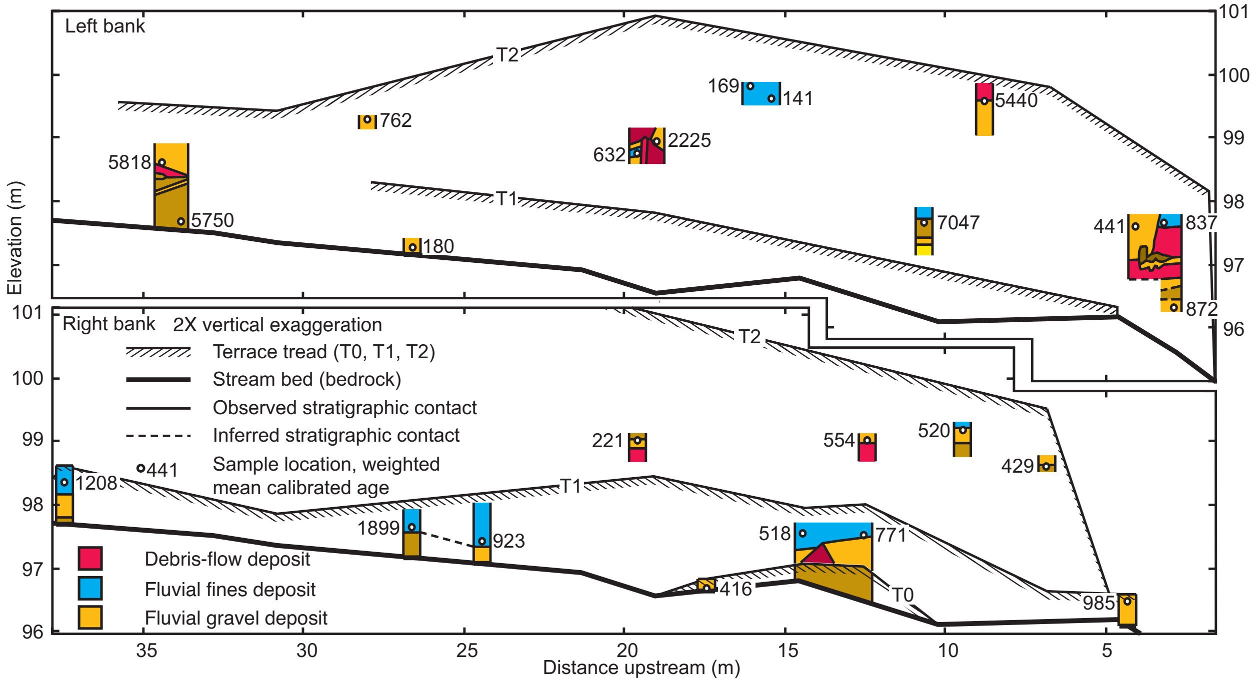

810
811

Figure 5

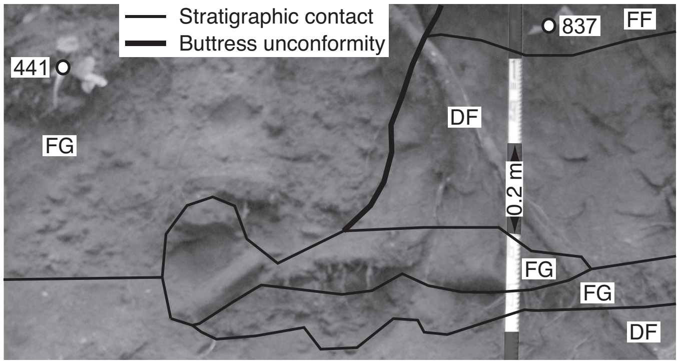
Stratigraphic contact
Buttress unconformity
441
837
FF
FG
DF
0.2 m
FG
FG
DF

Figure 6

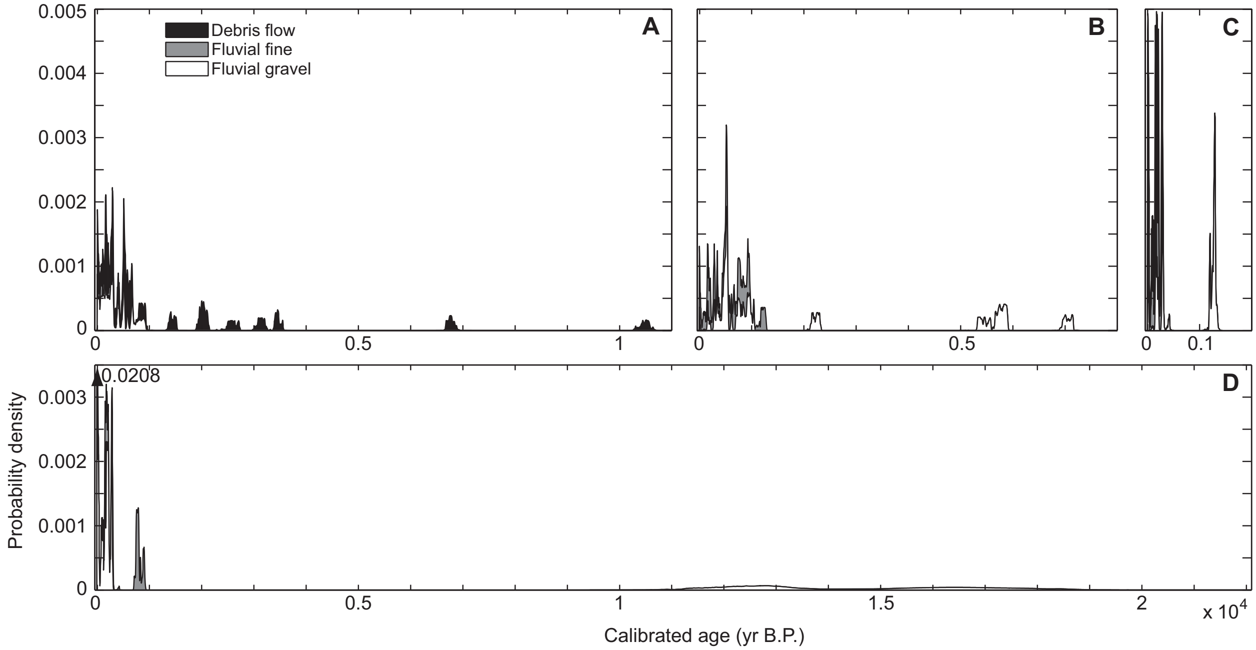
Debris flow
Fluvial fine
Fluvial gravel
A
B
C
D
0.005
0.004
0.003
0.002
0.001
0
0.5
1
0.1
0.0208
Probability density
1.5
2
x 10^4
Calibrated age (yr B.P.)

815 **Figure 7**

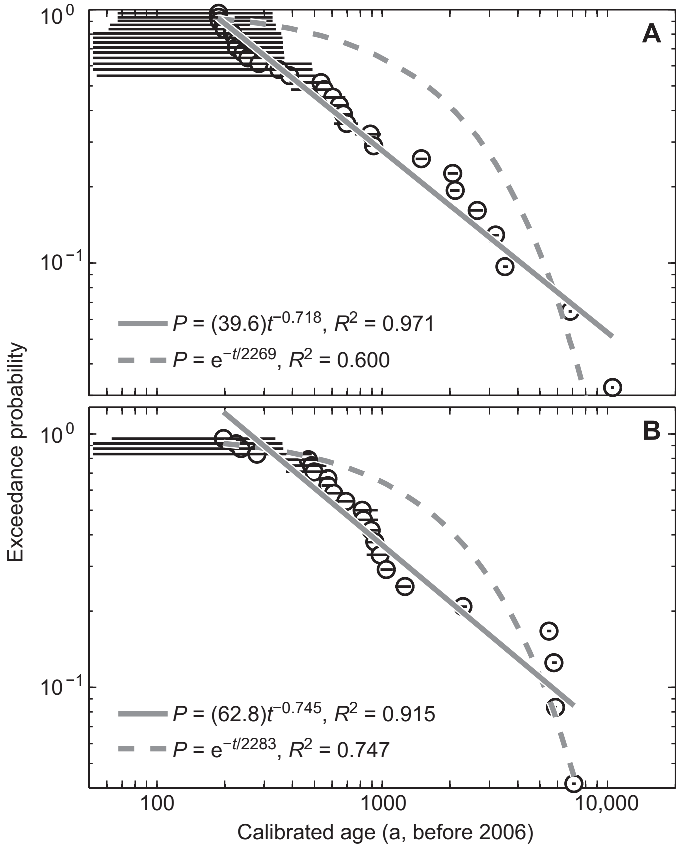

816